Journal of Physics: Condensed Matter

Intermediate-range order in vitreous SiO_2 and GeO_2

To cite this article: Shinji Kohara and Kentaro Suzuya 2005 *J. Phys.: Condens. Matter* **17** S77

View the article online for updates and enhancements.

You may also like

- Solution-based coating and printing of polycrystalline Ge films using GeO_2 solution by moderate-pressure hydrogen plasma reduction
Hiromasa Ohmi, Kiyoshi Yasutake and Hiroaki Kakiuchi
- Reliability assessment of germanium gate stacks with promising initial characteristics
Cimang Lu, Choong Hyun Lee, Tomonori Nishimura et al.
- Germanium CMOS potential from material and process perspectives: Be more positive about germanium
Akira Toriumi and Tomonori Nishimura

This content was downloaded from IP address 193.205.210.83 on 13/08/2024 at 16:59

INSTITUTE OF PHYSICS PUBLISHING JOURNAL OF PHYSICS: CONDENSED MATTER

J. Phys.: Condens. Matter **17** (2005) S77–S86 doi:10.1088/0953-8984/17/5/009

Intermediate-range order in vitreous SiO_2 and GeO_2

Shinji Kohara[1] **and Kentaro Suzuya**[2]

[1] Japan Synchrotron Radiation Research Institute, 1-1-1 Kouto, Mikazuki-cho, Sayo-gun, Hyogo 679-5198, Japan
[2] Neutron Science Research Center, Japan Atomic Energy Research Institute (JAERI), Tokai, Naka, Ibaraki 319-1195, Japan

Received 3 December 2004, in final form 3 December 2004
Published 21 January 2005
Online at stacks.iop.org/JPhysCM/17/S77

Abstract

The total structure factors, $S(Q)$, obtained from high-energy x-ray and neutron diffraction measurements on vitreous SiO_2 (v-SiO_2) and vitreous GeO_2 (v-GeO_2) have been analysed by the reverse Monte Carlo (RMC) modelling technique to generate a three-dimensional structural model. The bond angle distributions and the ring size distributions from the model indicated that the sixfold ring and six- and sevenfold rings are dominant in v-SiO_2 and v-GeO_2, respectively. However, the fraction of threefold rings of Ge in v-GeO_2 is larger than that of Si in v-SiO_2 glass. These features are consistent with the published neutron diffraction and Raman scattering studies.

1. Introduction

Vitreous SiO_2 (v-SiO_2) and vitreous GeO_2 (v-GeO_2) are two prototype oxide glasses containing SiO_4 and GeO_4 tetrahedra, respectively, as units of short-range order. Despite much research on v-SiO_2 and v-GeO_2 using for example diffraction [1–6], NMR study [7, 8], Raman spectroscopy [9], molecular dynamics (MD) simulation [10, 11], RMC simulation [12–14], and so on, the structural differences between the two typical glasses, particularly for the intermediate-range order (IRO) that arises from a continuous three-dimensional network [15] consisting of corner-sharing tetrahedra, have not been definitively discriminated.

Important quantitative structural information on short- and intermediate-range order in glasses can be obtained from the atom distribution functions derived using x-rays and neutron diffraction (ND). High-energy x-rays and a pulsed neutron source in particular provide detailed and reliable structural information with high resolution in real space due to a wide range of scattering vector Q. Furthermore, in order to obtain more realistic and useful structural information from the diffraction data, particularly for IRO, modelling techniques are necessary. Reverse Monte Carlo (RMC) modelling [16, 17] allows a quantitative fit of the experimental data without the use of potential functions. In comparison with MD and/or standard Monte Carlo simulation techniques, RMC is particularly useful for the study of multicomponent glasses for which the determination of interatomic potential functions for chemical bonding is difficult.

 © 2005 IOP Publishing Ltd Printed in the UK

In this study, IRO structures of v-SiO_2 and v-GeO_2 have been investigated by RMC modelling using a combination of high-energy x-rays and published neutron diffraction data [6, 18]. In particular, we focused on the ring structure in terms of the determination of the bond angle distribution and the ring size distribution.

2. Experimental details

The high-energy x-ray diffraction (HEXRD) experiments were carried out at the bending magnet beamline, BL04B2 [19] of SPring-8 with a two-axis diffractometer for disordered materials [20]. Incident photon energies of 61.7 keV for v-SiO_2 and 113.8 keV for v-GeO_2 were obtained from a bent Si(220) crystal and a bent Si(111) crystal with a third harmonic, respectively. The x-ray diffraction patterns of 2 mm thick flat plates of v-SiO_2 and v-GeO_2 were measured in a symmetrical transmission geometry. The details of the experiments have been described elsewhere [20, 21].

3. Reverse Monte Carlo modelling

The RMC method has been shown to be a useful tool for constructing a three-dimensional structural model of disordered materials using mainly experimental diffraction data. In the RMC simulation technique, the atoms in an initial configuration are moved so as to minimize the deviation from experimental structural data, e.g., in this study, a combination of the high-energy x-ray and neutron diffraction data, using a standard Metropolis Monte Carlo algorithm.

The starting configurations were generated using hard-sphere Monte Carlo (HSMC) simulations with constraints applied to avoid physically unrealistic structures. The constraints were of two kinds: closest atom–atom approach and connectivity. The choices of the closest atom–atom approach were determined to avoid unreasonable spikes in the partial pair correlation functions. The constraints on the Si–O and Ge–O network connectivity were that all oxygen atoms were coordinated to two silicon and germanium atoms and that all silicon and germanium atoms were coordinated to four oxygen atoms. RMC simulations were then simultaneously performed for a system containing 3000 atoms, using the x-ray- and neutron-weighted interference function, $Q[S(Q) - 1]$. The box lengths were chosen to correspond to the number densities of 0.0662 $Å^{-3}$ for v-SiO_2 and 0.0627 $Å^{-3}$ for v-GeO_2.

4. Results

4.1. Structure factor $S(Q)$

The x-ray- and neutron-weighted interference functions, $Q[S^{X}(Q) - 1]$ and $Q[S^{N}(Q) - 1]$, of v-SiO_2 [22] and v-GeO_2 are shown in figures 1 and 2, respectively. The experimental interference functions of these glasses exhibit significant oscillations up to the maximum measured Q value of 35 $Å^{-1}$, while there is a large difference between the x-ray and neutron interference functions in the Q range from 1 to 11 $Å^{-1}$ due to the differences in weighting factors, as follows:

$$\text{v-SiO}_2\text{: } S^{X}(Q) = 0.218S_{SiSi}(Q) + 0.498S_{SiO}(Q) + 0.284S_{OO}(Q), \quad (1)$$

$$S^{N}(Q) = 0.069S_{SiSi}(Q) + 0.388S_{SiO}(Q) + 0.543S_{OO}(Q), \quad (2)$$

$$\text{v-GeO}_2\text{:}S^{X}(Q) = 0.444S_{GeGe}(Q) + 0.444S_{GeO}(Q) + 0.112S_{OO}(Q), \quad (3)$$

$$S^{N}(Q) = 0.171S_{GeGe}(Q) + 0.485S_{GeO}(Q) + 0.344S_{OO}(Q), \quad (4)$$

where it is assumed that atomic form factor $f(Q)$ may be approximated by the atomic number. These equations demonstrate that x-ray diffraction data are necessary to study the intermediate-

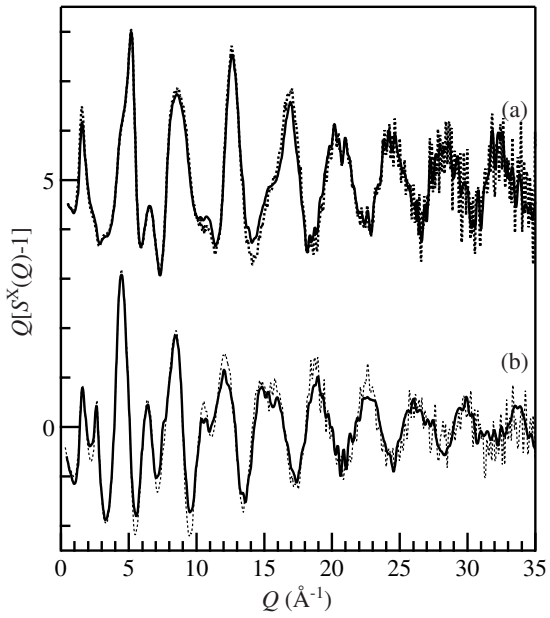

Figure 1. X-ray-weighted interference functions, $Q[S^X(Q) - 1]$, of (a) v-SiO_2 [22] and (b) v-GeO_2. Dotted curves, experimental data; solid curves, RMC model. v-SiO_2 data are displaced upward by five units for ease of viewing.

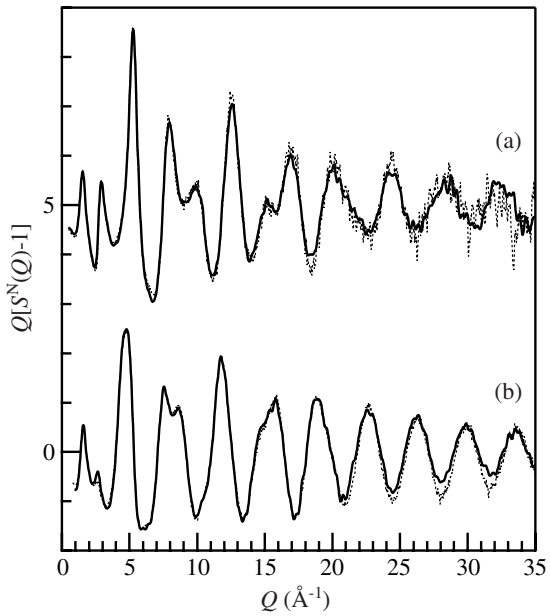

Figure 2. Neutron-weighted interference functions, $Q[S^N(Q) - 1]$, of (a) v-SiO_2 [22] and (b) v-GeO_2. Dotted curves, experimental data; solid curves, RMC model. v-SiO_2 data are displaced upward by five units for ease of viewing.

range order of oxide glasses, because the weighting factors of the Si–Si and Ge–Ge correlations, which are strongly related to the IRO of these glasses, are larger for x-rays than for neutrons.

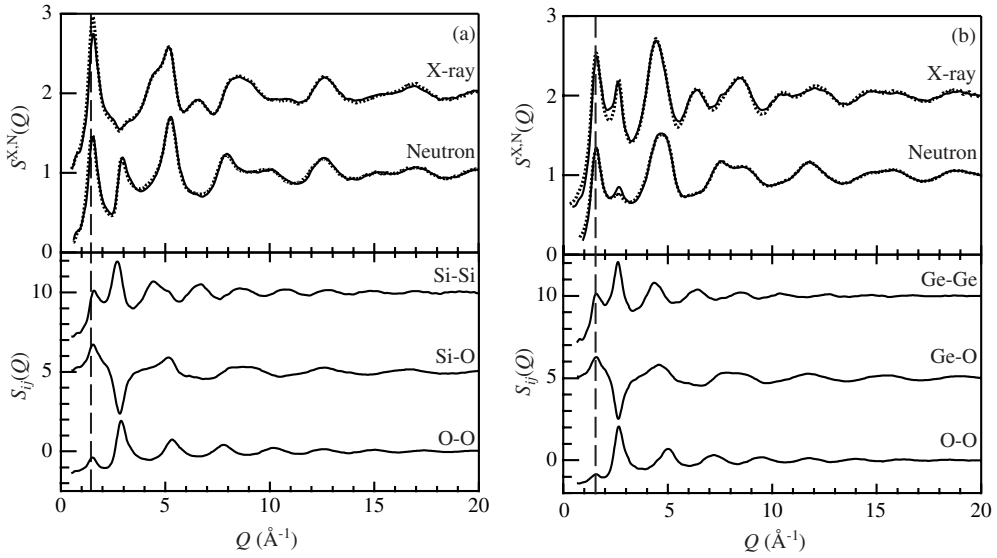

Figure 3. Total and partial structure factors, $S^{X,N}(Q)$ and $S_{ij}(Q)$, of (a) v-SiO_2 [22] and (b) v-GeO_2 derived from the RMC model. Dotted curves, experimental data; solid curves, RMC model. Successive curves are displaced upward for ease of viewing. The dashed curves are guides for the eye.

The experimental interference functions were well reproduced by RMC in a wide range of scattering vector Q.

Figure 3 shows the total and partial structure factors, $S^{X,N}(Q)$ and $S_{ij}(Q)$, of v-SiO_2 [22] and v-GeO_2, respectively. The first sharp diffraction peak (FSDP) observed at $Q \sim 1.55$ Å^{-1} implies the presence of IRO due to the cages formed by the topological connection of the tetrahedral units in the network [23], because the FSDP shows up as a positive feature in all three partial structure factors of both glasses at $Q \sim 1.55$ Å^{-1} in figure 3. In the case of v-SiO_2, all partial structure factors show good agreement with the results of MD simulation using interaction potentials that include two- and three-body contributions [10]. However, $S_{OO}(Q)$ of v-GeO_2, derived from a combination of neutron diffraction and anomalous x-ray scattering, shows a negative feature at the FSDP position [5, 24], whereas a positive feature is found at the FSDP position in all three partial structure factors obtained by RMC modelling using neutron diffraction and anomalous x-ray scattering data [14].

4.2. Pair distribution function $g(r)$

The experimental x-ray- and neutron-weighted pair-distribution functions, $g^{X,N}(r)$, of v-SiO_2 [22] and v-GeO_2 are shown in figure 4.

The differences between the x-ray and neutron weighting factors provide a more exact separation of complex atom–atom correlations in real space. Furthermore, the neutron-weighted pair-distribution functions, $g^{N}(r)$, of the RMC model agree well with the experimental data, hence the RMC model should be able to provide relatively reliable structural information.

Yuan and Cormack [11] recently reported the total correlation functions of v-SiO_2 using MD simulation. They used the two-body potential from van Beest *et al* (BKS) [27] and the three-body potentials from Vessal *et al* (VSL) [28], modified by Smith *et al* [29]. The VSL model yields two distinct peaks, 3.7 and 4.2 Å, in the Si–O second correlation, whereas the

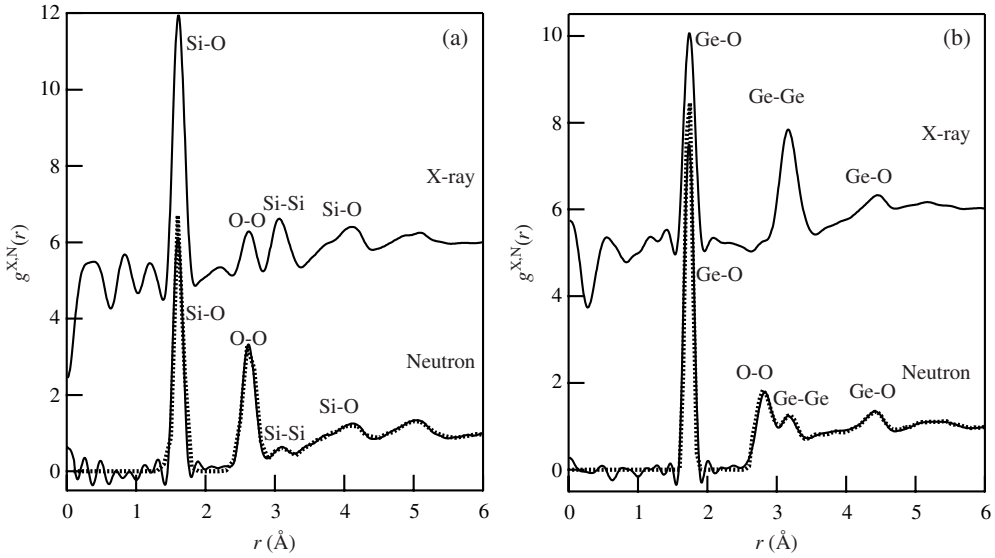

Figure 4. The x-ray- and neutron-weighted pair-distribution functions, $g^{X,N}(r)$, of (a) v-SiO_2 [22] and (b) v-GeO_2. Solid curves, experimental data; dotted curves, RMC model. The x-ray data are displaced upward by five units for ease of viewing. $Q_{max} = 33$ Å^{-1}. Lorch [25] and modified Welch [26] modification functions were used for x-ray and neutron data, respectively.

BKS model yields a peak at 4.2 Å and a shoulder at 3.7 Å. Our x-ray- and neutron-weighted pair distribution functions show shoulder peaks at 3.7 Å. However, as shown in [22], partial pair distribution functions of Si–O, $g_{Si-O}(r)$, derived using the RMC model, do not have such a distinct peak. Yuan and Cormack pointed out that the shoulder at 3.7 Å is associated mainly with the width of the Si–O–Si bond angle distribution, so further discussion will be described in the following section.

4.3. Intermediate-range order in RMC model

The bond angle distributions of v-SiO_2 [22] and v-GeO_2 are shown in figure 5 with those of v-B_2O_3 [30]. The O–Ge–O and O–Si–O bond angle distributions show a maximum close to the value of 109.4° expected for a regular tetrahedron. The O–B–O and B–O–B bond angle distributions show a maximum of around 120°, suggesting the existence of the boroxol ring (threefold ring of B). This interpretation is also supported by the sharp peak at 60° of the B–B–B and O–O–O bond angle distributions. The Si–Si–Si bond angle distribution shows peaks at around 60° (threefold ring of Si) and 80°–150° (four- to eightfold ring of Si), respectively. In addition, the Si–O–Si bond angle distribution has a maximum of around 150°. These features suggest that the threefold ring is a minor group of ring structures. This is consistent with the results of Raman scattering and first-principles MD studies [31–33]. On the other hand, the threefold ring fraction in the Ge–Ge–Ge bond angle distribution is larger than that in v-SiO_2. The Ge–O–Ge bond angle distribution shows a maximum of around 130° (close to 120°), which suggests a relatively large fraction of threefold rings. This interpretation is supported by the existence of a peak at around 25° in the Ge–Ge–O bond angle distribution, which is a smaller angle than that of around 15° for the peak in the Si–Si–O bond angle distribution and very similar to the B–B–O distribution for v-B_2O_3 (threefold ring of B). The bond angle distribution in our RMC model for v-SiO_2 is generally in agreement with the results of another RMC study [12], except for details of the Si–Si–Si and Si–O–Si bond angle distributions. As

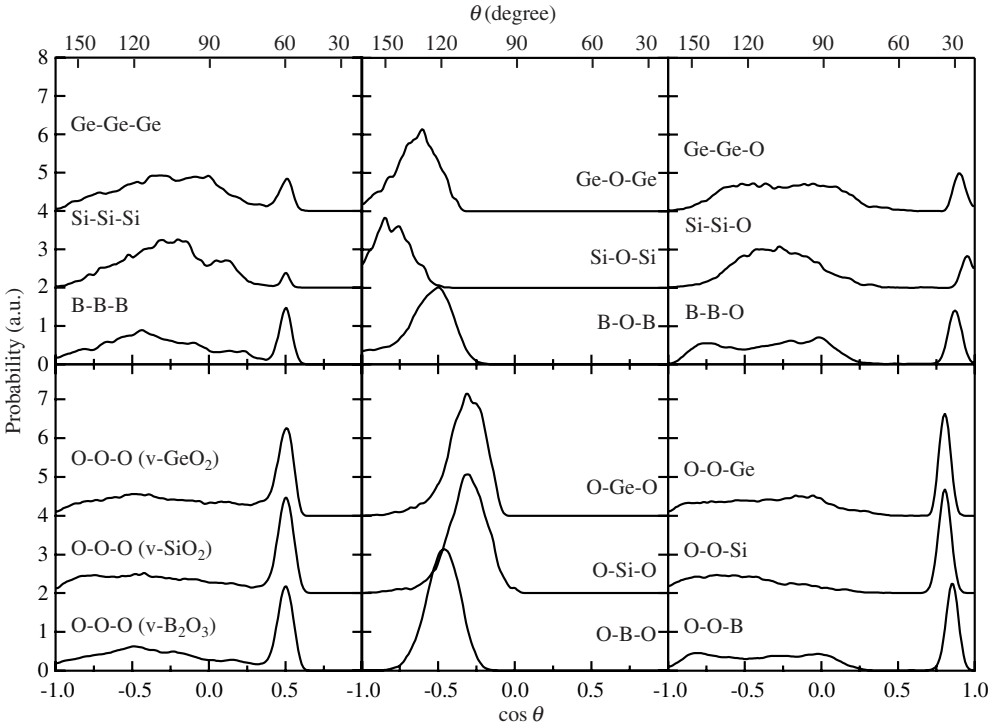

Figure 5. The bond angle distributions of v-GeO_2, v-SiO_2 [22], and v-B_2O_3 [30]. Successive curves are displaced upward by two units for ease of viewing.

can be seen in figure 5, our results show well defined peaks at 60°, 80°, and 105°. In the Si–Si–Si bond angle distribution, and 150° in the Si–O–Si bond angle distribution, whereas the model obtained by another RMC study does not have enough statistics concerning the Si–Si–Si and Si–O–Si bond angle distributions. No well defined peak is observed in the Si–O–Si bond angle distribution. These detailed features of Si–Si–Si and Si–O–Si bond angle distributions are consistent with the data obtained by MD simulation [10]. In the other RMC model, x-ray and neutron diffraction data up to $Q_{\max} = 20$ and 43 Å^{-1}, respectively, were used, while we used the x-ray-weighted structure factor up to $Q_{\max} = 35$ Å^{-1} and obtained better agreement with experimental data than in the RMC study. In addition, the partial pair-distribution functions, $g_{\mathrm{SiSi}}(r)$ and $g_{\mathrm{OO}}(r)$, reported in [12] have unreasonable spike peaks, whereas, as can be seen in figure 3 and [22], our results do not have such an unreasonable spike peak. As discussed in [22], the weighting factor of the Si–Si correlation is larger for x-rays than for neutrons, so that our model well reproduces the x-ray-weighted total structure factor $S^{\mathrm{X}}(Q)$ up to high Q because it contains more reliable structural information for the Si–Si correlation. Hence our Si–Si–Si bond angle distribution, which is strongly related to IRO of the glass, should be more reliable than the results in [12].

The most probable bond angle (MPBA) and fwhm for the Si–O–Si bond angle distribution derived using the RMC model is shown, together with previous data, in table 1. Our RMC model provides the values of MPBA = 146° and fwhm = 17°, which are consistent with the analytical results determined from a combination of high-energy x-ray diffraction and neutron diffraction data [3], but are slightly larger those of many crystalline silicates [36]. Yuan and Cormack suggested, on the basis of a comparison of BKS and VLS models with

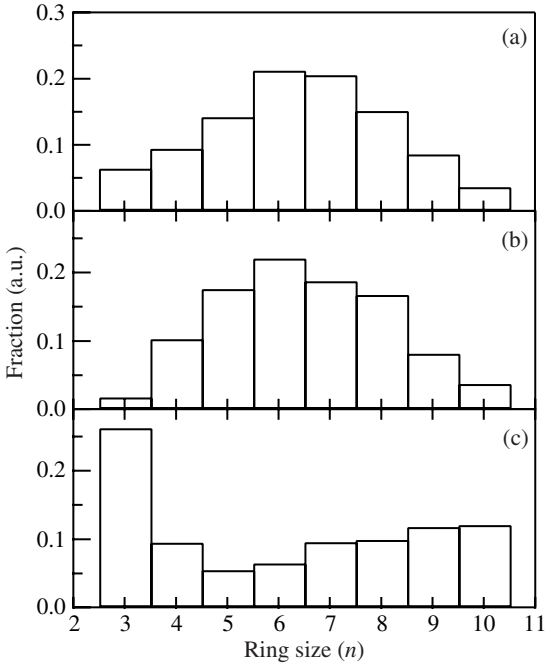

Figure 6. The ring size distributions of (a) v-GeO_2, (b) v-SiO_2 [22], and (c) v-B_2O_3.

Table 1. Comparison of Si–O–Si bond angle distributions obtained using different methods. (Note: the VKRE is MD simulation with the three-body potential from Vashishta *et al* [37].)

	RMC/HEXRD/ND This work	BKS [11]	VSL [11]	VKRE [37]	RMC/ND [34]	XRD [35]	HEXRD [2]	HEXRD/ND [3]	NMR [8]
MPBA (deg)	146	152	147	142	146	144	147	147	142
fwhm (deg)	17	36	9.7	25	21	38	35	17	26

partial correlation functions, that a broad Si–O–Si bond angle distribution leaves a smooth shoulder (Si–second O correlation) at 3.7 Å and a narrower Si–O–Si bond angle distribution exhibits a pronounced shoulder. However, our RMC model produced the smoother shoulder at 3.7 Å for the pair distribution function and narrow Si–O–Si bond angle distribution. This may be due to the contributions of high-energy x-ray diffraction data up to high Q, which has a large weighting factor for Si–Si correlation.

The bond angle distributions for v-GeO_2, obtained using another RMC model, have been reported [14]. This other RMC model was obtained using Ge-edge anomalous x-ray scattering and neutron diffraction data up to $Q_{max} = 15$ Å^{-1}; hence, the peaks of the bond angle distributions for Ge–O–Ge and O–Ge–O are broader than those in our results. We also applied two sets of experimental data, neutron and high-energy x-ray diffraction data up to $Q_{max} = 35$ Å^{-1}. The IRO of v-SiO_2 and v-GeO_2 is a result of the connections of SiO_4 and GeO_4 tetrahedra, respectively, so that the RMC model, which can reproduce the experimental structure factor up to high Q, particularly for x-rays, provides more detailed and more reliable structural information.

The ring size distributions calculated using the configurations of v-SiO_2 [22], v-GeO_2, and v-B_2O_3 [30] are shown in figure 6. The size distribution of v-B_2O_3 has a maximum at $n = 3$, indicating that the boroxol ring (threefold ring of B) structure is dominant. The v-SiO_2

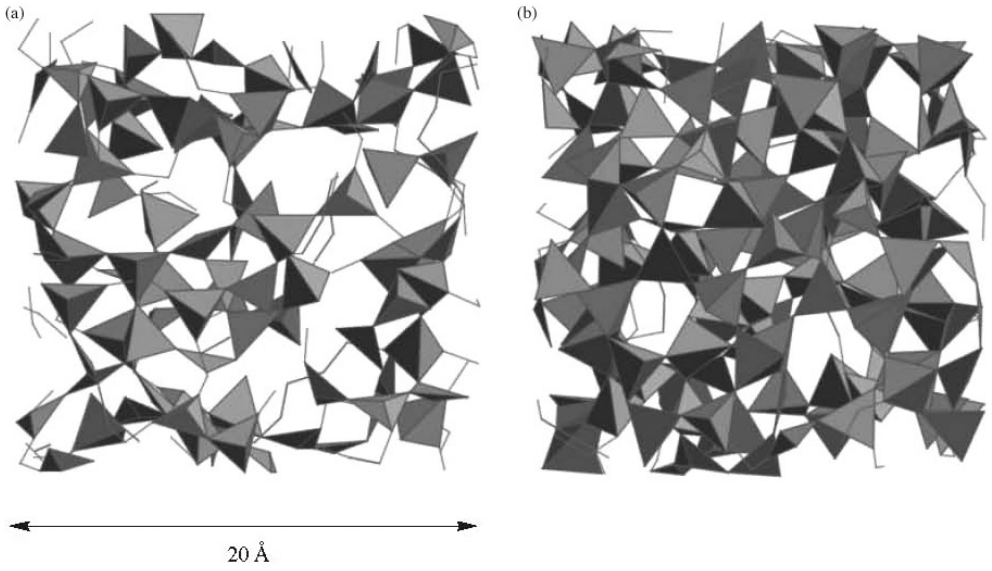

Figure 7. A 10 Å thick slice of part of the largest RMC-produced configurations of (a) v-SiO_2 and (b) v-GeO_2.

ring size distribution has a maximum at $n = 6$, which is in agreement with the results obtained by MD simulation [37], though the fraction of $n = 6$ is slightly larger than that of other ring sizes in the MD results. The ring size distribution of v-GeO_2 has large fractions at $n = 6$ and 7, which indicates that six- and sevenfold rings of Ge are dominant, but the fraction of threefold rings in v-GeO_2 is larger than that in v-SiO_2. These features are consistent with the conclusions based on the neutron diffraction [4] and Raman scattering [9] data.

Such differences in the ring statistics or the bond angle distributions between v-SiO_2 and v-GeO_2 are partially established in the initial models generated by HSMC simulations. However, the initial models cannot reproduce the experimental diffraction data at all, and the details of ring statistics of the initial models are different from those in figure 6. In order to confirm the differences of ring statistics between v-SiO_2 and v-GeO_2, RMC simulations were performed for each, using the atomic configuration of the other as the initial configuration. We obtained a reasonable structural model that can reproduce both the x-ray and neutron diffraction data for v-GeO_2, where the fraction of threefold rings became larger than that in the initial configuration taken from the RMC model for v-SiO_2. On the other hand, we could not obtain a reasonable structural model that reproduces both the x-ray and neutron diffraction data for v-SiO_2. These results suggest that a model with a large fraction of threefold rings is unfit for the diffraction data of v-SiO_2, whereas for v-GeO_2, which has a relatively large fraction of threefold rings, it is consistent with the diffraction data. In other words, these observations suggest that the intermediate-range structures, such as the ring statistics of v-SiO_2 and v-GeO_2, essentially differ, and that the determination of an exact ring size distribution in this manner is unexpectedly sensitive to experimental diffraction data.

Figure 7 represents 20 Å thick sections of the RMC configuration for v-SiO_2 and v-GeO_2. It is obvious that SiO_4 and GeO_4 tetrahedra are well reproduced. Furthermore, all tetrahedra were connected at the corner site of O. This chemically reasonable and almost defect-free (no-dangling-bond) model indicates that the differences in the ring size distributions between v-SiO_2 and v-GeO_2 are essential structural differences between typical tetrahedral-network glasses.

5. Conclusions

Reverse Monte Carlo modelling with a combination of high-energy x-ray and neutron diffraction data up to $Q_{max} = 35$ Å^{-1} was carried out to obtain reliable structural models of v-SiO_2 and v-GeO_2. The RMC model reproduces well two structure factors that have different weighting factors for each correlation, and could provide relatively detailed and reliable structural information. High-energy x-ray data are necessary to study the IRO of v-SiO_2 and v-GeO_2, because of the large weighting factors of Si–Si and Ge–Ge correlations for x-rays, which have a strong influence on the Si–Si–Si, Ge–Ge–Ge, Si–O–Si, and Ge–O–Ge bond angle distributions. The RMC study indicates that the sixfold ring of Si is dominant in v-SiO_2, while the fraction of threefold rings of Ge is higher in v-GeO_2 than in v-SiO_2. The structural models of v-SiO_2 and v-GeO_2 obtained by RMC modelling should be standard models for studying the mixed alkali glass and pressure-reserved glass from room temperature to high temperature.

Acknowledgments

The authors are grateful to Dr I Sakai for experimental assistance and to Dr A C Hannon and Professor A C Wright for providing us with the neutron diffraction data for vitreous GeO_2. Discussion with Dr R L McGreevy is gratefully appreciated.

References

[1] Wright A C 1994 *J. Non-Cryst. Solids* **179** 84
[2] Poulsen H F, Neuefeind J, Neumann H-B, Schneider J R and Zeidler M D 1995 *J. Non-Cryst. Solids* **188** 63
[3] Neuefeind J and Liss K-D 1996 *Ber. Bunsenges. Phys. Chem.* **100** 1341
[4] Desa J A E, Wright A C and Sinclair R N 1988 *J. Non-Cryst. Solids* **99** 276
[5] Price D L, Saboungi M-L and Barns A C 1998 *Phys. Rev. Lett.* **81** 3207
[6] Stone C E, Hannon A C, Ishihara T, Kitamura N, Shirakawa Y, Sinclair R N, Umesaki N and Wright A C 2001 *J. Non-Cryst. Solids* **293–295** 769
[7] Dupree R and Pettifer R F 1984 *Nature* **308** 523
[8] Pettifer R F, Dupree R, Farnan I and Sternberg U 1988 *J. Non-Cryst. Solids* **106** 408
[9] Durben D J and Wolf G H 1991 *Phys. Rev.* B **43** 2355
[10] Vashishta P, Kalia R K, Rino J P and Ebbsjö I 1990 *Phys. Rev.* B **41** 12197
[11] Yuan X and Cormack A N 2003 *J. Non-Cryst. Solids* **319** 31
[12] Keen D A 1997 *Phase Transit.* **61** 109
[13] Keen D A and Dove M T 1999 *J. Phys.: Condens. Matter* **11** 9263
[14] Kang S, Park C, Saito M and Waseda Y 1999 *Mater. Trans. JIM* **40** 552
[15] Zachariasen W H 1932 *J. Am. Chem. Soc.* **54** 3841
[16] McGreevy R L and Pusztai L 1988 *Mol. Simul.* **1** 359
[17] McGreevy R L 2001 *J. Phys.: Condens. Matter* **13** R877
[18] Suzuya K, Price D L, Saboungi M-L and Ohno H 1997 *Nucl. Instrum. Methods* B **133** 57
[19] Isshiki M, Ohishi Y, Goto S, Takeshita K and Ishikawa T 2001 *Nucl. Instrum. Methods* A **467/468** 663
[20] Kohara S, Suzuya K, Kashihara Y, Matsumoto N, Umesaki N and Sakai I 2001 *Nucl. Instrum. Methods* A **467/468** 1030
[21] Kohara S and Suzuya K 2003 *Nucl. Instrum. Methods* B **199** 23
[22] Kohara S and Suzuya K 2002 *Phys. Chem. Glasses* **43C** 51
[23] Wright A C, Hulme R A, Grimley D I, Sinclair R N, Martin S W, Price D L and Galeener F L 1991 *J. Non-Cryst. Solids* **129** 213
[24] Waseda Y, Sugiyama K, Matsubara E and Harada K 1990 *Mater. Trans. JIM* **31** 421
[25] Lorch E A 1969 *J. Phys. C: Solid State Phys.* **2** 229
[26] Press W H, Teukolsky S A, Vetterling W T and Flannery B P 1992 *NUMERICAL RECEPES in FORTRAN: The Art of Scientific Computing* 2nd edn (Cambridge: Cambridge University Press)
[27] van Beest B W H, Kramer G J and van Santen R A 1990 *Phys. Rev. Lett.* **64** 1955

[28] Vessal B, Amini M, Fincham D and Catlow C R A 1989 *Phil. Mag.* B **60** 753
[29] Smith W, Greaves G N and Gillan M J 1995 *J. Chem. Phys.* **103** 3091
[30] Suzuya K, Yoneda Y, Kohara S and Umesaki N 2000 *Phys. Chem. Glasses* **41** 282
[31] Galeener F L 1982 *Solid State Commun.* **44** 1037
[32] Pasquarello A and Car R 1998 *Phys. Rev. Lett.* **80** 5145
[33] Umari P, Gonze X and Pasquarello A 2003 *Phys. Rev. Lett.* **90** 027401
[34] Gladden L F 1992 *The Physics of Non-Crystalline Solids* ed L D Pye, W C LaCourse and H J Stevens (London: Taylor and Francis) p 91
[35] Mozzi R L and Warren B E 1969 *J. Appl. Crystallogr.* **2** 164
[36] Gibbs G V 1982 *Am. Mineral.* **67** 421
[37] Rino J P, Ebbsjö I, Kalia R K, Nakano A and Vashishta P 1993 *Phys. Rev.* B **47** 3053